Multicomponent Interdiffusion and Self-Diffusion of the Cationic Poly{[9,9-bis(6′-*N*,*N*,*N*-trimethylammonium)hexyl]fluorene-phenylene} Dibromide in a Dimethyl Sulfoxide + Water Solution[†]

María Monteserín,[‡] María J. Tapia,[‡] Ana C. F. Ribeiro,[§] Cecília I. A. V. Santos,[§] Artur J. M. Valente,*[,§] Hugh D. Burrows,*[,§] Ricardo Mallavia,[||] Markus Nilsson,[⊥] and Olle Söderman[⊥]

Departamento de Química, Universidad de Burgos, Plaza Misael Bañuelos, Burgos 09001, Spain, Departamento de Química, Universidade de Coimbra, 3004-535 Coimbra, Portugal, Instituto de Biología Molecular y Celular, Universidad Miguel Hernández, Elche 03202, Alicante, Spain, and Physical Chemistry 1, Center for Chemistry and Chemical Engineering, Lund University, P.O. Box 124, SE 221 00 Lund, Sweden

The diffusion behavior of the conjugated polyelectrolyte poly{[9,9-bis(6′-*N*,*N*,*N*-trimethylammonium)hexyl]-fluorene-phenylene} bromide (HTMA-PFP) with different molecular weights has been studied in dimethyl sulfoxide (DMSO) + water solutions. Samples of HTMA-PFP with various molecular weights were obtained by synthesis of poly[9,9-bis(6′-bromohexyl)fluorene-phenylene] via a Suzuki coupling reaction, characterized by size exclusion chromatography (SEC), and quaternized with trimethylamine. Multicomponent chemical interdiffusion coefficients (mutual diffusion coefficients) were determined for solutions of HTMA-PFP and DMSO in water using the Taylor dispersion method. The results suggest specific interactions between the DMSO and the polymer. In addition, these systems were studied by pulse-field gradient nuclear magnetic resonance spectroscopy (PFG-NMR), and the corresponding self-diffusion coefficients were obtained. These were modeled using the Kirkwood−Riseman model, and a good fit to the observed behavior was obtained using literature data for molecular dimensions.

Introduction

There is increasing interest in conjugated polyelectrolytes as advanced materials with actual or potential applications in areas such as chemical or biological sensors,[1,2] electron-transport or injection layers,[3,4] photovoltaic systems,[5,6] and light-emitting diodes (LEDs)[1] and electrochemical cells (LECs).[7] The presence of ionic groups confers solubility in water or polar organic solvents,[8] making them attractive for solution processing, which is valuable for the preparation of devices using solvent-based techniques such as inkjet or screen printing.[3,9] In addition, these conjugated polyelectrolytes may self-assemble with oppositely charged species to form novel nanostructures for optoelectronical or other applications.[10–12]

Polymers and copolymers containing fluorene moieties are particularly valuable because of their high fluorescence quantum yields, blue emission, and tendency to form ordered structures.[13–15] However, conjugated polyelectrolytes based on polyfluorenes and related copolymers are rigid-rod polymers that have low solubility in water and tend to form clusters in aqueous solution. This can be counteracted by the use of organic cosolvents[16,17] or nonionic surfactants.[18–24] Cationic fluorene-phenylene and related alternating copolymers are proving particularly attractive and being used in areas such as probes or sensors for nucleic acids[14,15] and surfactants.[25] In addition, they show excellent properties for use as electron-transporting and hole-blocking layers in devices.[26,27] Many of these properties can be modulated by changing the counterions.[1,26] This can be related to the difference in interaction between the conjugated polyelectrolyte and the counterion, as seen through the thermophysical properties.[28] Similar effects of the counterion are seen in the optoelectronic properties of other conjugated polyelectrolytes.[29] The condensation of oppositely charged ions with rigid-rod conjugated polyelectrolytes, such as those containing poly(*p*-phenylene) [including poly(fluorene)] backbones, is also of considerable theoretical interest.[30,31] However, there are very little literature data on how counterions bind with this class of compounds in solution. In part this is due to the very low concentrations normally needed to study this class of compounds. One notable exception is a report of osmotic coefficients of a cationic poly(phenylene) having chloride and iodide counterions,[32] where it was shown that it is possible to treat the qualitative features of the system in dilute solution using the classical Poisson−Boltzmann (PB) model of ion association[33,34] rather than the Manning−Oosawa treatment, commonly used for ion condensation with flexible polyelectrolytes.[35,36] However, the PB model fails at the more quantitative level, indicating the need for both better theoretical models and more experimental data.

Diffusion behavior may help obtain an understanding of interactions with these systems. Thus, we have studied the interdiffusion and intradiffusion (self-diffusion) behavior of the cationic poly{[9,9-bis(6′-*N*,*N*,*N*-trimethylammonium)hexyl]fluorene-phenylene} bromides (HTMA-PFP) with different molecular weights. These have been studied in dimethyl sulfoxide (DMSO) + water solutions,[14,25] because of the low solubility of HTMA-PFP in water due to cluster formation.[25,37] Interdiffusion, also called mutual diffusion, occurs in the presence of

---

[†] Part of the "Josef M. G. Barthel Festschrift".

* Corresponding authors. E-mail address: avalente@ci.uc.pt (A.J.M.V.); burrows@ci.uc.pt (H.D.B.).

[‡] Universidad de Burgos.

[§] Universidade de Coimbra.

[||] Universidad Miguel Hernández.

[⊥] Lund University.

10.1021/je900875w

Scheme 1

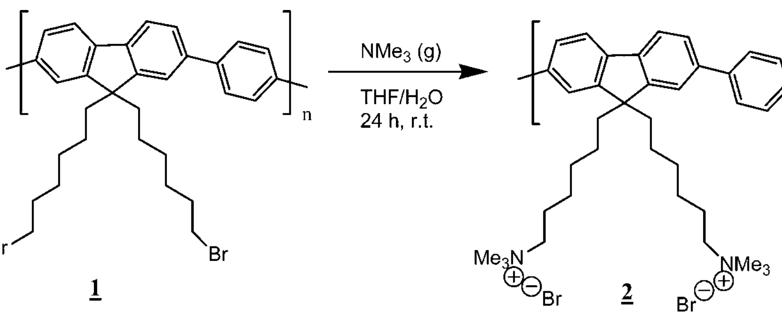

Table 1. Molecular Weights of Different Batches of the Polymer 1 and the Corresponding Data Calculated for Polymer 2[a]

batch of polymer **1**	$\bar{M}_n$[b] kg·mol^{-1}	PDI[c]	$\bar{M}_p$[d] kg·mol^{-1}	n[e]	batch of polymer **2**	$\bar{M}_p$[d] kg·mol^{-1}	$\bar{M}_n$[b] kg·mol^{-1}
P1	12.0	1.9	20.8	37	S1	25.3	14.5
P2	24.9	2.1	36.0	64	S2	43.8	30.1
P3[f]	50.7	2.4	81.1	143[g]	S3[f]	97.9	61.3

[a] Corrected using the same PS calibration. [b] Number average molecular weight. [c] Polydispersity index. [d] Maximum peak molecular weight. [e] Number of repeat units per chain. [f] Bimodal distribution components obtained by Gaussian deconvolutions of the experimental data: P3 (90.7 % with $\bar{M}_n = 58.8$ kg·mol^{-1}, PDI = 2.08, and 9.3 % with $\bar{M}_n = 13.7$ kg·mol^{-1}, PDI = 1.09); and corresponding S3 (highest fraction with $\bar{M}_n = 71.1$ kg·mol^{-1} and lowest one with $\bar{M}_n = 16.6$ kg·mol^{-1}) components. [g] A second distribution is also present with $n = 36$.

a binary or multicomponent system with a gradient in the chemical potential. Intradiffusion (self-diffusion), in contrast, refers to the interchange of labeled or unlabeled species under conditions of uniform chemical composition.[38] These results allow an estimation of the degree of counterion dissociation.

Additional interest in this work comes from the fact that the diffusion behavior of multicomponent chemical systems under conditions relevant to various applications (e.g., chemical or biological sensors) is still poorly understood; in particular, there is strong interest in the diffusion behavior of ternary systems.[39] However, no data is available in literature for ternary systems involving rigid conjugated polyelectrolytes, such as HTMA-PFP, in mixed solvents (DMSO + water, in this case). Thus, the purpose of this work has been to measure ternary mutual diffusion coefficients for 298.15 K at carrier concentrations from (0.000 to 2.020·10^{-6}) mol·dm^{-3} (in terms of repeat units) and (0.068 to 0.282) mol·dm^{-3}, for HTMA-PFP ($\bar{M}_n = 30.1$ kg·mol^{-1}) and DMSO, respectively, by using the Taylor dispersion method,[40] helping us to better understand the structure of these systems. In addition, the effect of molecular weight on the tracer diffusion of HTMA-PFP has been measured by the Taylor dispersion technique.

We have also studied the self-diffusion[41] of the polymer chain using the powerful and well-established pulse-field gradient NMR (PFG-NMR) technique.[42]

Experimental Section

Synthesis of Poly{[9,9-bis(6′-N,N,N-trimethylammonium)-hexyl]fluorene-phenylene} bromide. Neutral poly[9,9-bis(6′-bromohexyl)fluorene-phenylene] (**1**) was synthesized via a Suzuki coupling reaction using 1,4-phenyldiboronic acid and 2,7-dibromo-9,9-bis(6′-bromohexyl)fluorine.[43] Copolymer **1** was made water-soluble by treatment with excess trimethylamine gas at room temperature (the Menschutkin reaction), which converts the alkyl bromide of the polymer side chain into its corresponding cationic quaternized tetraalkylammonium group: poly{[9,9-bis(6′-*N*,*N*,*N*-trimethylammonium)hexyl]fluorene-phenylene} bromide (polymer **2** in Scheme 1); for details on the polymerization and purification, see ref 44. We assume, in agreement with previous reports,[45] the almost quantitative conversion of the copolymer **1** into **2** and that this does not affect the degree of polymerization. NMR data support this (see Supporting Information, characterization, and Figures SI-1 to SI-5 for further details).

Three different batches of the neutral polymer **1** were prepared by slightly varying the synthesis procedure. The lowest molecular weight polymer batch (P1) was synthesized via a Suzuki coupling reaction carried out over 3 days. For the other two batches (P2 and P3) the reaction was carried out using different palladium catalysts[46] and was stopped after 12 h. The molecular weights of the three batches of the neutral polymer **1** were characterized by size exclusion chromatography (SEC) in tetrahydrofuran (THF) as solvent using polystyrene standards for calibration. The results are summarized in the Table 1. The batch with the highest molecular weight polymer (P3) shows a bimodal distribution (Supporting Information, Figure SI-5) with 90.7 % of the fraction with $\bar{M}_n = 58.8$ kg·mol^{-1}, $n = 143$, and 9.3 % of the fraction with $\bar{M}_n = 13.7$ kg·mol^{-1}, $n = 36$. The molecular weights of polymer **2** (S1, S2, and S3, shown in Table 1) were calculated using the degree of polymerization of the chain determined experimentally for polymer **1** (P1, P2, and P3) and the corresponding repeat unit molecular weight (684.6 g·mol^{-1}). For the highest molecular weight polymer (S3) slight differences in the bimodal distribution may be observed with respect to the precursor polymer **1** (P3) as a consequence of the synthesis and purification processes. For this reason this polymer batch will mainly be used for comparison with the lower molecular weight systems.

Reagents and Solutions. For diffusion experiments, polymer **2** samples of three molecular weights $\bar{M}_n$ = (14.5, 30.1, and 61.3) kg·mol^{-1}, for S1, S2, and S3, respectively, were used. Solutions were prepared in mixtures of DMSO (1) + H_2O (2) and DMSO (1) + D_2O (2′), with solvent volume fractions equal to $\phi_1 = 0.04$ and $\phi_1 = 0.70$, for multicomponent interdiffusion and self-diffusion experiments, respectively. These were all prepared by weighting and left stirring overnight. Concentrations (in terms of repeat units) of polymeric solutions are (6.65, 6.44, and 6.71)·10^{-3} mol·kg^{-1} (for S1 to S3, respectively). All of the solutions were prepared with a concentration uncertainty of less than ± 0.1 %.

The solubility of polymer **2** is dependent on the DMSO + water ratio volume and from the HTMA-PFP emission quantum yield we suggest that the maximum solubility for the highest molecular weight polymer (S3) is for a solvent volume fraction of about $\phi_1 = 0.70$, while the other two molecular weight batches show very similar behavior between about $\phi_1 = 0.10$ and $\phi_1 = 0.80$ (see Supporting Information, Figure SI-6, for further details).

All of the experiments were carried out at 298.15 K.

Polymer Characterization Techniques. ^{1}H and ^{13}C NMR spectra were recorded on a Bruker Avance 500 spectrometer, with tetramethylsilane as an internal reference. Fourier transform infrared (FTIR) spectra were obtained using a Nicolet model 520P spectrometer with samples prepared as KBr pellets. Coupled SEC and light scattering measurements were carried out using a HP-1090 liquid chromatograph with an autosampler, autoinjector, and ELSD 2000 Alltec evaporative light scattering detector (ELSD). SEC was carried out using THF as eluent, and data were calibrated using Polymer Laboratories EasiCal PS standards using two-column PLGel of 5 μm at constant room temperature.

Taylor Dispersion Technique. The Taylor dispersion technique has been extensively described in literature;[40,47–49] for convenience we will describe the relevant points related with the method which allow the computation of ternary diffusion coefficients, D_{11}, D_{22}, D_{12}, and D_{21}. Here D_{ik} represents the mutual diffusion coefficient of species *i* in the presence of a concentration gradient of *k*.

Diffusion in a ternary solution is described by the diffusion equations

$$-(J_1) = (D_{11})_v \frac{\partial c_1}{\partial x} + (D_{12})_v \frac{\partial c_2}{\partial x} \tag{1}$$

$$-(J_2) = (D_{21})_v \frac{\partial c_1}{\partial x} + (D_{22})_v \frac{\partial c_2}{\partial x} \tag{2}$$

where J_1, J_2, $(\partial c_1)/(\partial x)$, and $(\partial c_2)/(\partial x)$ are the molar fluxes and the gradients in the concentrations of solute 1 and 2, respectively. Main diffusion coefficients, D_{11} and D_{22}, give the flux of each solute produced by its own concentration gradient. Cross diffusion coefficients D_{12} and D_{21} give the coupled flux of each solute driven by a concentration gradient of the other solute. A positive D_{ik} cross-coefficient ($i \neq k$) indicates cocurrent coupled transport of solute *i* from regions of higher concentration of solute *k* to regions of lower concentration. However, a negative D_{ik} coefficient indicates counter-current coupled transport of solute *i* from regions of lower to higher concentration of solute *k*.

Extensions of the Taylor technique have been used to measure ternary mutual diffusion coefficients (D_{11}, D_{22}, D_{12}, and D_{21}) for multicomponent solutions. These coefficients are evaluated by fitting the ternary dispersion equation (eq 3) to two or more replicate pairs of peaks for each carrier stream.

$$V(t) = V_0 + V_1 t + V_{\max}(t_R/t)^{1/2}\left[W_1 \exp\left(-\frac{12D_1(t - t_R)^2}{r^2 t}\right) + (1 - W_1)\exp\left(-\frac{12D_2(t - t_R)^2}{r^2 t}\right)\right] \tag{3}$$

Two pairs of refractive-index profiles, D_1 and D_2, are the eigenvalues of the matrix of the ternary D_{ik} coefficients.

In these experiments, for finite concentrations, small volumes of ΔV of solution, of composition $\bar{c}_1 + \Delta\bar{c}_1$ and $\bar{c}_2 + \Delta\bar{c}_2$ are injected into carrier solutions of composition $\bar{c}_1$ and $\bar{c}_2$ at time $t = 0$. $\Delta\bar{c}_1$ and $\Delta\bar{c}_2$ are lower than ($1.7 \cdot 10^{-5}$ and 1.28) mol$\cdot$dm^{-3}, respectively.

Analysis of ternary diffusion coefficients in the limit of zero polymer concentration shows that this corresponds to the binary diffusion of aqueous DMSO, and in this limit D_{11} corresponds to the tracer diffusion of polymer in supporting DMSO solutions, as has been described elsewhere.[50] Consequently, the tracer diffusion coefficients of polymer (component 1) dissolved in supporting DMSO (component 2) solutions, D_{11}^{T} ($c_1/c_2 = 0$), were obtained by injecting small volumes (ΔV) of solution, of composition $\bar{c}_1 + \Delta\bar{c}_1$ and $\bar{c}_2 + \Delta\bar{c}_2$ into carrier solutions of composition $\bar{c}_1 = 0$ and $\bar{c}_2 \neq 0$ at time $t = 0$. The tracer diffusion coefficients of DMSO in supporting polymer solutions, that is, D_{22}^{T} ($c_2/c_1 = 0$), were not measured, on the basis of the observation that the polymer is only dissolved, at the molecular level, in the presence of DMSO.

^{1}H NMR Self-Diffusion Measurements. A Bruker DMX-200 NMR spectrometer, equipped with a field gradient probe unit, was used to measure the self-diffusion coefficients of polymer by following the ^{1}H resonance of the $N(CH_3)_3$ group at 2.95 ppm (Supporting Information, Figure SI-4). The stimulated echo pulse was used following the recommended procedure reported elsewhere.[42]

For the pulse sequence, the gradient strength (g) was changed from (0 to 9.63) T$\cdot$m^{-1}, and the duration of the gradient pulse (δ) was varied between (1.4 and 2.1)$\cdot 10^{-3}$ s. The diffusion time (the time between leading edges of the field gradient pulses, Δ) was typically 20 ms.

^{1}H NMR self-diffusion experiments of the cationic polymer **2** were carried out on solutions with polymer concentrations (in terms of repeat units) around $6 \cdot 10^{-3}$ mol$\cdot$kg^{-1} in DMSO + D_2O ($\phi_1 = 0.70$) solution.

Experimental Results and Discussion

For clarity this section is organized into two subsections, one for the measurement of the mutual diffusion coefficients and the second for self-diffusion coefficients. In the conclusions section we will show how these give indications on the degree of counterion dissociation.

Multicomponent-Diffusion Coefficients. A Taylor dispersion apparatus was used to measure diffusion coefficients for the ternary system HTMA-PFP, S2, (1) + DMSO (2) + water at 298.15 K at different concentration ratios. The average diffusion coefficients (D_{11}, D_{22}, D_{12}, and D_{21}) of each carrier solution, determined from four profiles generated by injecting samples that were either more or less concentrated than the carrier solution, are shown in Table 2. At least 99 % reproducibility was obtained with all measurements.

The main diffusion coefficients D_{11} and D_{22} give the molar fluxes of the polymer (1) and DMSO (2) components driven by their own concentration gradient. It is possible to observe (from Table 2) that there is a trend for these diffusion coefficients to decrease upon increasing both S2 polymer and DMSO concentrations. The data can be fitted to a second-degree polynomial concentration function. Extrapolating to zero HTMA-PFP and DMSO concentration, the corresponding mutual diffusion coefficients at infinitesimal concentration, D_{11}^0 and D_{22}^0, can be calculated and are equal to (0.438 ($\pm$ 0.005) and 1.14 ($\pm$ 0.04))$\cdot 10^{-9}$ m$^2\cdot$s^{-1}, respectively. It is worth mentioning that D_{22}^0 is equal to the Taylor binary diffusion coefficients of aqueous 0.282 mol$\cdot$dm^{-3} DMSO, which we have measured, and to the published DMSO binary diffusion coefficient,[51] which strongly supports the validity of the methodology used.

Table 2. Ternary Diffusion Coefficients for Aqueous HTMA-PFP (S2) (1) + DMSO (2), at 298.15 K[a]

C_1 / $\mathrm{mol \cdot dm^{-3}}$	C_2 / $\mathrm{mol \cdot dm^{-3}}$	D_{11} (± s)[b] / $10^{-9}\ m^2 \cdot \mathrm{s}^{-1}$	D_{12} (± s) / $10^{-9}\ m^2 \cdot \mathrm{s}^{-1}$	D_{21} (± s) / $10^{-9}\ m^2 \cdot \mathrm{s}^{-1}$	D_{22} (± s) / $10^{-9}\ m^2 \cdot \mathrm{s}^{-1}$
$5.09 \cdot 10^{-7}$	0.068	0.42 (± 0.02)	≈ 0	4589 (± 555)	1.12 (± 0.04)
$1.08 \cdot 10^{-6}$	0.141	0.40 (± 0.01)	≈ 0	902 (± 107)	1.11 (± 0.04)
$1.53 \cdot 10^{-6}$	0.198	0.39 (± 0.04)	≈ 0	138 (± 16)	1.11 (± 0.04)
$2.02 \cdot 10^{-6}$	0.282	0.37 (± 0.04)	≈ 0	−485 (± 45)	1.11 (± 0.04)

[a] Polymer concentrations given in terms of repeat units. [b] s is the standard deviation of the average value.

Table 3. Tracer Diffusion Coefficients, D^{T}_{11}, D^{T}_{12}, D^{T}_{21}, and D^{T}_{22}, of Polymer (S1, S2, or S3) (1) + DMSO (2) in Aqueous Solutions, at 298.15 K

polymer	D^{T}_{11} (± s)[a] / 10^{-10} $m^2 \cdot \mathrm{s}^{-1}$	D^{T}_{12} (± s)[b] / 10^{-9} $m^2 \cdot \mathrm{s}^{-1}$	D^{T}_{21} (± s) / 10^{-9} $m^2 \cdot \mathrm{s}^{-1}$	D^{T}_{22} (± s) / 10^{-9} $m^2 \cdot \mathrm{s}^{-1}$
S1	4.1 (± 0.1)	0	18910 (± 10253)	1.12 (± 0.02)
S2	4.9 (± 0.8)	0	15767 (± 10123)	1.14 (± 0.06)
S3	4.3 (± 0.1)	0	8579 (± 5586)	1.14 (± 0.06)

[a] s is the standard deviation of the average value. [b] For this system, keep in mind that the limiting values of cross-coefficients D_{12} should be zero.

From the analysis of cross-coefficient values for finite concentrations we have found that (a) the polymer transport is not affected by the presence of a DMSO gradient ($D_{12} \approx 0$) and (b) there is a strong dependence of D_{21} on DMSO (or polymer) concentration, and D_{21} decreases upon increasing those concentrations. It should be stressed that a negative D_{21} value gives a clear indication of a counter-flux of DMSO in the presence of high concentrations of polymer, as has been noted previously.[52]

This diffusion-coefficient behavior can be explained by the existence of strong interactions between DMSO and polymer; at low polymer concentrations some of the DMSO molecules interact with polymer (specific solvation), decreasing the effective number of DMSO molecules available to diffuse, and consequently the D_{21} increases. As polymer concentration increases, the amount of DMSO needed to solubilize it increases; consequently the effect of DMSO surrounding the polymer becomes dominant, producing conditions for the occurrence of a DMSO counter-flux. Specific interactions between various organic cosolvents and conjugated polyelectrolytes have previously been demonstrated in an anionic fluorene-phenylene copolymer using spectroscopic and photophysical measurements, coupled with molecular dynamics simulations.[17] Support for a similar mechanism of preferential interaction between polymer and DMSO comes from tracer diffusion (see discussion below) and molecular dynamic simulation (see Figure SI-7 in Supporting Information).

If we consider that D_{12}/D_{22} gives the number of moles of polymer cotransported per mole of DMSO, we may say that, at the concentrations used, a mole of diffusing DMSO does not transport any significant amount of polymer. However, through D_{21}/D_{11} values, at the same concentrations, we can expect that a mole of diffusing polymer cotransports at most $1 \cdot 10^4$ mol of DMSO ($c_1 = 0.509 \cdot 10^{-3}\ \mathrm{mol \cdot dm^{-3}}$, $c_2 = 0.068\ \mathrm{mol \cdot dm^{-3}}$), decreasing the cotransport with the increase of its concentration, until the opposite situation is obtained, that is, a mole of diffusing polymer counter-transports $1.3 \cdot 10^3$ mol of DMSO. This is similar to the behavior previously described by Leaist and MacEwan.[52]

The effect of HTMA-PFP molecular weight on the tracer diffusion coefficients has also been studied. Table 3 gives the diffusion coefficients, D^{T}_{11}, D^{T}_{12}, D^{T}_{21}, and D^{T}_{22}, of the ternary systems at 298.15 K, that is, polymer (S1, S2, and S3) at tracer concentration in DMSO + water solutions.

D^{T}_{11} and D^{T}_{22} can be considered to be independent of the molecular weight of polymer, while D^{T}_{12} is independent of DMSO. It is worth pointing out that D^{T}_{22} and D^{0}_{22} are equal and the values of D^{T}_{11} and D^{0}_{11} are very close ((4.9 and 4.4)$\cdot 10^{-10}$ $\mathrm{m^2 \cdot s^{-1}}$, respectively) as should be expected. We believe that this agreement between the tracer and the mutual diffusion at infinitesimal concentration (obtained from different experiments) guarantees the self-consistency of the methodology used.

The parameter D^{T}_{21}, which gives the effect of polymer on the DMSO transport, decreases upon increasing the molecular weight, providing support to the above discussion. The decrease of D^{T}_{21} with an increase of polymer molecular weight can be explained by an increase of the interaction between polymer and DMSO.

Self-Diffusion Coefficients. The HTMA-PFP self-diffusion coefficients were determined by using PFG-NMR. The influence of molecular weight polydispersity in PFG-NMR self-diffusion experiments of polymers has been discussed by several authors.[53,54] We follow the ideas on the application of the technique to study polydisperse polymer systems discussed by Hakansson et al.[53] For polymers S1 and S2, assuming that a polydisperse polymer will give a distribution of self-diffusion coefficients, the signal attenuation in a PFG-NMR experiment is given by

$$I_n = \int P(D^*) \exp(-kD^*)\, \mathrm{d}D^* \qquad (4)$$

where $P(D^*)$ is the probability of finding a component with self-diffusion coefficient D^* and $P(D^*)$ can be described as a log-normal distribution

$$P(D^*) = \frac{1}{D^* \sigma \sqrt{2\pi}} \exp\left(-\frac{[\ln(D^*) - \ln(D_0{}^*)]^2}{2\sigma^2}\right) \qquad (5)$$

where $D_0{}^*$ is the median of the distribution and σ is a measure of the width of the distribution. These parameters can be obtained from the experimental signal decays by fitting experimental data with eqs 4 and 5: see Figure 1.

From this distribution, the average diffusion coefficient $\langle D^* \rangle$ is calculated from

$$\langle D^* \rangle = D_0{}^* \exp\left(\frac{\sigma^2}{2}\right) \qquad (6)$$

and the corresponding data are shown in Table 4.

With polymer S3, there is clear evidence from the size exclusion chromatograms for a bimodal average molecular weight distribution with two polymer populations (90.7 % of $\bar{M}_n = 71.1\ \mathrm{kg \cdot mol^{-1}}$ and 9.3 % of $\bar{M}_n = 16.6\ \mathrm{kg \cdot mol^{-1}}$, Table 1 and Supporting Information, Figure SI-5). Consequently, the S3 echo decay is expected to require a biexponential kinetic analysis:[55]

$$I = I_0\left\{P_1 \exp\left[-\gamma^2 g^2 \delta^2\left(\Delta - \frac{\delta}{3}\right)D_s^*\right] + P_2 \exp\left[-\gamma^2 g^2 \delta^2\left(\Delta - \frac{\delta}{3}\right)D_f^*\right]\right\} \tag{7}$$

where D_s^* and D_f^* are self-diffusion coefficients for polymer fractions with the highest (P_1) and lowest (P_2) molecular weights and γ is the proton magnetogyric ratio. Using eq 7, we obtained a D_s^* value of $3.1 \cdot 10^{-12}$ $m^2 \cdot s^{-1}$ for the $\bar{M}_n = 71.1$ $kg \cdot mol^{-1}$ fraction and a D_f^* value of $1.54 \cdot 10^{-11}$ $m^2 \cdot s^{-1}$ for the $\bar{M}_n = 16.6$ $kg \cdot mol^{-1}$ fraction of S3 sample.

Two different routes were used to theoretically analyze the ^1H NMR diffusion results. In the first case, the average diffusion coefficient $\langle D^* \rangle$ of the samples with a normal chromatographic size distribution (S1 and S2) and the slow and fast components (D_s^* and D_f^*) of the sample with a bimodal distribution (S3) were related to the sample molecular weight through a scaling equation, while with the second model, $\langle D^* \rangle$ values of S1 and S2 and D_s^* and D_f^* values of S3 were used to obtain structural parameters of the polymer and confirm the cylindrical hairy rod structure for polymer **2** on the basis of the Kirkwood−Riseman model for translational diffusion.

The dependence of the self-diffusion coefficient on the average polymer molecular weight can be given by the empirical equation[56]

$$D^* = K\bar{M}_n^{\ -\upsilon} \tag{8}$$

where K and υ are scaling parameters. To ensure that the scaling parameters are constants, the use of eq 8 is limited, in the case of polydisperse systems, to a dilute solution regime.

Fitting the experimental self-diffusion coefficients of S1 and S2 to eq 8 and assuming $\upsilon = 1$, as expected for a rod-like polymer structure, we obtain $K = 2.6\ (\pm\ 0.2) \cdot 10^{-10}$ $kg \cdot m^2 \cdot s^{-1} \cdot mol^{-1}$. For these conjugated polyelectrolytes, self-diffusion coefficients can thus be used as a direct measurement of the molecular weight. For the case of the sample S3 (with a bimodal average molecular weight distribution) a good fit to eq 9 is obtained introducing the self-diffusion coefficients, for the slow and fast components as shown in Figure 2 (○). This suggests that the diffusion behavior of all three polymer samples can be scaled with the inverse of molecular weights. We note that, in a NMR self-diffusion study of poly(*p*-phenylene ethynylene)s in dilute solutions, a rather lower value of υ (= 0.71) is observed, suggesting semiflexible rod-like chains.[57] We do not have a sufficient range of samples to test whether this is also the case for our system, but small-angle neutron scattering data on a closely related alternating copolymer[21] and other structural studies on fluorene-based polymers[58] strongly support the idea of a rigid fluorene phenylene backbone.

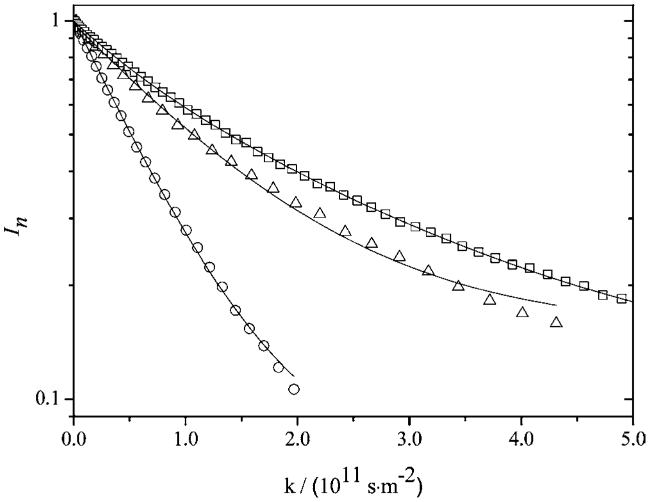

Figure 1. PFG-NMR echo decay for the $N(CH_3)_3$ resonance of the three polymers: ○, S1; △, S2; □, S3. Solid lines were obtained by fitting eqs 4 and 5 for S1 and S2 and eq 7 for S3 to normalized echo-decay intensities (see text for further details).

Table 4. Effect of Polymer 2 Molecular Weight on Self-Diffusion Coefficients

polymer **2**	$\bar{M}_n$ $kg \cdot mol^{-1}$	D_0^* $m^2 \cdot s^{-1}$	$\langle D^* \rangle$ $m^2 \cdot s^{-1}$	$D_{s,f}^*$ $m^2 \cdot s^{-1}$
S1	14.5	$1.52 \cdot 10^{-11}$	$1.72 \cdot 10^{-11}$	
S2	30.1	$6.85 \cdot 10^{-12}$	$1.01 \cdot 10^{-11}$	
S3	16.6			$1.54 \cdot 10^{-11}$
	71.1			$3.1 \cdot 10^{-12}$

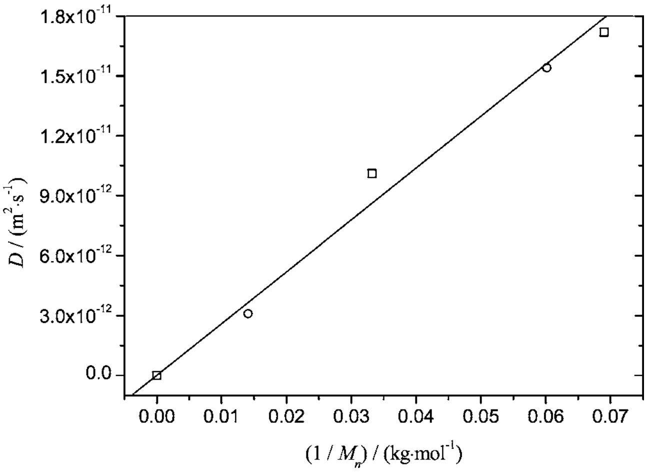

Figure 2. Self-diffusion coefficients plotted against the inverse of $\bar{M}_n$. □, the experimental average diffusion coefficients values $\langle D^* \rangle$ for S1 and S2; ○, the median of the distribution, D_0^*, for the fast and slow components of S3. The straight line is the theoretical plot obtained using the Kirkwood−Riseman model (eq 9), using literature values for polymer dimensions, as discussed in the text.

If we consider that fluorene-based polymers and copolymers can be treated as rigid rods,[59] diffusion coefficients can be estimated from the appropriate modification of the Stark−Einsten equation for the case of cylinders.[60] For simplicity, we have used the Kirkwood−Riseman model,[60] which can be expressed as:

$$D_{KR} = \frac{k_B T}{3\pi\eta L_w}\ln(L_w/b) \tag{9}$$

where the contour length (L_w) is given by the monomer unit length (l_m) multiplied by the number of repeat units per chain [$L_w = n \cdot l_m$, and $n = \bar{M}_n/(684.6\ g \cdot mol^{-1})$], while b is the thickness, k_B is the Boltzmann's constant, T is the temperature in Kelvin, and η is the viscosity of this solvent mixture for DMSO + D_2O, $\phi_1 = 0.70$. Since the physical properties of DMSO−water are not related linearly to those of each constituent, values of viscosity have to be taken for this composition ($\eta = 3.73 \cdot 10^{-3}$ Pa·s at 298.15 K).[61] The repeat unit length for fluorene-phenylene alternating copolymers ($l_m = 0.1125$ Å), involving effectively three 1,4-phenylene units, was taken as 3/2 times the literature fluorene monomer length, using data from ref 62. The best fit to eq 9 of experimental self-diffusion coefficients data [$\langle D^* \rangle$ for S1 and S2 and the slow and fast components (D_s^* and D_f^*) for S3; see Figure 2] was obtained using a thickness of $b = 12$ Å, which seems physically realistic considering contributions of 7.6 Å for the length of a fully stretched hexyl chain, 3 Å from the radius of the $N(CH_3)_3$

headgroup (assuming that the trimethylammonium headgroup can be modeled as a sphere with a volume of 100 Å^3),[63] with the remaining contribution being due to the thickness of the aromatic backbone (cf. Scheme 1).

Although the quality of the agreement with the experimental data is possibly fortuitous, the fact that there is an excellent correspondence over a nearly two-fold increase in molecular weight using only literature parameters strongly supports the application of the Kirkwood−Riseman model to this system, confirming a cylindrical, hairy rod structure for polymer **2** in this medium.

Conclusions

A study has been made of the multicomponent and self-diffusion coefficients of three different molecular weight samples of a cationic fluorene-based conjugated polyelectrolyte in DMSO−water solutions. Self-diffusion coefficients are proportional to the reciprocal of molecular weights of the polymer for the polymer samples with a normal molecular weight distribution. With the self-diffusion coefficients, the behavior can be modeled using the simple Kirkwood−Riseman model for the polymers with a normal average molecular weight distribution assuming a rod-like structure for the polymer. Using a contour length for the repeat unit from the literature, the diameter of the rods can be calculated from the experimental average diffusion coefficients and Kirkwood−Riseman model. In principle, it should be possible to estimate the degree of counterion binding from the multicomponent and self-diffusion coefficients. As a first approximation, we use a two-state model for counterion binding.[35,36] Details of the calculation are given as Supporting Information. While the application of this model is questionable for rigid-rod polyelectrolytes,[32,33,64] we believe that qualitatively it is informative on this important parameter, which is otherwise difficult to determine for these systems. The effective charge (i.e., the degree of counterion dissociation) of strongly charged polyelectrolytes is known to increase with concentration.[65,66] However, the concentrations used in these measurements correspond to the dilute solution limit, and within experimental error, the values of the polymer dissociation degrees obtained [$\alpha = 0.37\ (\pm\ 0.08)$] are virtually independent of polymer size. While the value of α is not given explicitly for the cationic poly(*p*-phenylene) polyelectrolyte studied by Ballauff et al.,[32] the values estimated from these calculations are fully consistent with those from osmotic pressure measurements in that study, ref 32, assuming the standard relationship between the osmotic coefficients and the degree of dissociation of polyelectrolytes.[67]

Note Added in Proof: After the acceptance of this paper, we found a relevant, very recent paper by Edman and co-workers,[68] in which they have used pulsed-field gradient NMR to study the aggregation of a very similar cationic conjugated polyelectrolyte in methanol solution. Our self-diffusion data are consistent with theirs for dilute solutions.

Supporting Information Available:

FTIR, proton, and ^{13}C NMR spectra of polymers **1** and **2**, SEC-ELSD chromatograms, HTMA-PFP fluorescence quantum yields as function of composition in DMSO + water, molecular dynamics simulations of HTMA-PFP trimers in DMSO + water ($\phi_1 = 0.04$), and estimation of the degree of counterion dissociation. This material is available free of charge via the Internet at http://pubs.acs.org.

Literature Cited

(1) Yang, R. Q.; Wu, H. B.; Cao, Y.; Bazan, G. C. Control of cationic conjugated polymer performance in light emitting diodes by choice of counterion. *J. Am. Chem. Soc.* **2006**, *128*, 14422–14423.

(2) Mauthner, G.; Landfester, K.; Kock, A.; Bruckl, H.; Kast, M.; Stepper, C.; List, E. J. W. Inkjet printed surface cell light-emitting devices from a water-based polymer dispersion. *Org. Electron.* **2008**, *9*, 164–170.

(3) Schubert, U. S. Ink-jet printing of functional polymers and materials: A (future) key technology in polymer science. *Macromol. Rapid Commun.* **2005**, *26*, 237–237.

(4) Decher, G. Fuzzy nanoassemblies: Toward layered polymeric multicomposites. *Science* **1997**, *277*, 1232–1237.

(5) Fendler, J. H. Chemical self-assembly for electronic applications. *Chem. Mater.* **2001**, *13*, 3196–3210.

(6) Tan, C. Y.; Alas, E.; Muller, J. G.; Pinto, M. R.; Kleiman, V. D.; Schanze, K. S. Amplified quenching of a conjugated polyelectrolyte by cyanine dyes. *J. Am. Chem. Soc.* **2004**, *126*, 13685–13694.

(7) Edman, L.; Liu, B.; Vehse, M.; Swensen, J.; Bazan, G. C.; Heeger, A. J. Single-component light-emitting electrochemical cell fabricated from cationic polyfluorene: Effect of film morphology on device performance. *J. Appl. Phys.* **2005**, *98*, 044502.

(8) Pinto, M. R.; Schanze, K. S. Conjugated polyelectrolytes: Synthesis and applications. *Synthesis* **2002**, 1293.

(9) Kawase, T.; Shimoda, T.; Newsome, C.; Sirringhaus, H.; Friend, R. H. Inkjet printing of polymer thin film transistors. *Thin Solid Films* **2002**, *438/439*, 279–287.

(10) Hoeben, F. J. M.; Pouderoijen, M. J.; Schenning, A.; Meijer, E. W. Energy transfer in chiral co-assemblies of triple hydrogen-bonded oligo(p-phenylene vinylene)s and porphyrin. *Org. Biomol. Chem.* **2006**, *4*, 4460–4462.

(11) Burrows, H. D.; Fonseca, S. M.; Dias, F. B.; de Melo, J. S.; Monkman, A. P.; Scherf, U.; Pradhan, S. Singlet Excitation Energy Harvesting and Triplet Emission in the Self-Assembled System Poly{1,4-phenylene-[9,9-bis(4-phenoxy-butylsulfonate)]fluorene-2,7-diyl} copolymer/tris(bipyridyl)ruthenium(II) in Aqueous Solution. *Adv. Mater.* **2009**, *21*, 1155–1159.

(12) Davies, M. L.; Burrows, H. D.; Moran, M. C.; Miguel, M. G.; Douglas, P. Cationic Fluorene-Based Conjugated Polyelectrolytes Induce Compaction and Bridging in DNA. *Biomacromolecules* **2009**, *10*, 2987–2997.

(13) Al Attar, H. A.; Monkman, A. P. Effect of surfactant on FRET and quenching in DNA sequence detection using conjugated polymers. *Adv. Funct. Mater.* **2008**, *18*, 2498–2509.

(14) Monteserín, M.; Burrows, H. D.; Valente, A. J. M.; Mallavia, R.; Di Paolo, R. E.; Maçanita, A. L.; Tapia, M. J. Interaction between Poly(9,9-bis(6′-*N*,*N*,*N*-trimethylammonium)hexyl)fluorene phenylene) Bromide and DNA as Seen by Spectroscopy, Viscosity, and Conductivity: Effect of Molecular Weights and DNA Secondary Structure. *J. Phys. Chem. B* **2009**, *113*, 1294–1302.

(15) Tapia, M. J.; Monteserin, M.; Valente, A. J. M.; Burrows, H. D.; Mallavia, R. *Adv. Colloid Interface Sci.* DOI: 10.1016/j.cis.2009.09.001.

(16) Wang, S.; Bazan, G. C. Solvent-dependent aggregation of a water-soluble poly(fluorene) controls energy transfer to chromophore-labeled DNA. *Chem. Commun.* **2004**, 2508–2509.

(17) Burrows, H. D.; Fonseca, S. M.; Silva, C. L.; Pais, A.; Tapia, M. J.; Pradhan, S.; Scherf, U. Aggregation of the hairy rod conjugated polyelectrolyte poly{1,4-phenylene-[9,9-bis(4-phenoxybutylsulfonate)]fluorene-2,7-diyl} in aqueous solution: an experimental and molecular modelling study. *Phys. Chem. Chem. Phys.* **2008**, *10*, 4420–4428.

(18) Burrows, H. D.; Lobo, V. M. M.; Pina, J.; Ramos, M. L.; de Melo, J. S.; Valente, A. J. M.; Tapia, M. J.; Pradhan, S.; Scherf, U. Fluorescence enhancement of the water-soluble poly{1,4-phenylene-[9,9-bis(4-phenoxybutylsulfonate)]fluorene-2,7-diyl} copolymer in n-dodecylpentaoxyethylene glycol ether micelles. *Macromolecules* **2004**, *37*, 7425–7427.

(19) Burrows, H. D.; Lobo, V. M. M.; Pina, J.; Ramos, M. L.; de Melo, J. S.; Valente, A. J. M.; Tapia, M. J.; Pradhan, S.; Scherf, U.; Hintschich, S. I.; Rothe, C.; Monkman, A. P. Interactions between surfactants and {1,4-phenylene-[9,9-bis(4-phenoxy-butylsulfonate)]-fluorene-2,7-diyl}. *Colloid Surf., A* **2005**, *270*, 61–66.

(20) Knaapila, M.; Almasy, L.; Garamus, V. M.; Pearson, C.; Pradhan, S.; Petty, M. C.; Scherf, U.; Burrows, H. D.; Monkman, A. P. Solubilization of polyelectrolytic hairy-rod polyfluorene in aqueous solutions of nonionic surfactant. *J. Phys. Chem. B* **2006**, *110*, 10248–10257.

(21) Burrows, H. D.; Knaapila, M.; Monkman, A. P.; Tapia, M. J.; Fonseca, S. M.; Ramos, M. L.; Pyckhout-Hintzen, W.; Pradhan, S.; Scherf, U. Structural studies on cationic poly{9,9-bis[6-(*N*,*N*,*N*-trimethylammonium) alkyl]fluorene-co-1,4-phenylene} iodides in aqueous solutions in the presence of the non-ionic surfactant pentaethyleneglycol monododecyl ether ($C_{12}E_5$). *J. Phys.: Condens. Matter* **2008**, *20*, 104210.

(22) Burrows, H. D.; Tapia, M. J.; Fonseca, S. M.; Valente, A. J. M.; Lobo, V. M. M.; Justino, L. L. G.; Qiu, S.; Pradhan, S.; Scherf, U.; Chattopadhyay, N.; Knaapila, M.; Garamus, V. Aqueous Solution Behaviour of Anionic Fluorene-co-thiophene Based Conjugated Polyelectrolytes. *ACS Appl. Mater. Interfaces* **2009**, *1*, 864–874.

(23) Burrows, H. D.; Tapia, M. J.; Fonseca, S. M.; Pradhan, S.; Scherf, U.; Silva, C. L.; Pais, A. A. C. C.; Valente, A. J. M.; Schillen, K.; Alfredsson, V.; Carnerup, A. M.; Tomsic, M.; Jamnik, A. Solubilization of Poly{1,4-phenylene-[9,9-bis(4-phenoxy-butylsulfonate)]fluorene-2,7-diyl} in Water by Non-ionic Amphiphiles. *Langmuir* **2009**, *25*, 5545–5556.

(24) Shi, S. Q.; Wudl, F. Synthesis and characterization of a water-soluble poly(para-phenylenevinylene) derivative. *Macromolecules* **1990**, *23*, 2119–2124.

(25) Monteserín, M.; Burrows, H. D.; Valente, A. J. M.; Lobo, V. M. M.; Mallavia, R.; Tapia, M. J.; García-Zubiri, I. X.; Di Paolo, R. E.; Maçanita, A. L. Modulating the emission intensity of poly-(9,9-bis(6′-*N*,*N*,*N*-trimethylammonium)hexyl)-fluorene phenylene) bromide through interaction with sodium alkylsulfonate surfactants. *J. Phys. Chem. B* **2007**, *111*, 13560–13569.

(26) Park, J.; Hoven, C. V.; Yang, R. Q.; Cho, N. S.; Wu, H. B.; Nguyen, T. Q.; Bazan, G. C. Photocurrent hysteresis by ion motion within conjugated polyelectrolyte electron transporting layers. *J. Mater. Chem.* **2009**, *19*, 211–214.

(27) Garcia, A.; Brzezinski, J. Z.; Nguyen, T. Q. Cationic Conjugated Polyelectrolyte Electron Injection Layers: Effect of Halide Counterions. *J. Phys. Chem. C* **2009**, *113*, 2950–2954.

(28) Ortony, J. H.; Yang, R.; Brzezinski, J. Z.; Edman, L.; Nguyen, T. Q.; Bazan, G. C. Thermophysical properties of conjugated polyelectrolytes. *Adv. Mater.* **2008**, *20*, 298–302.

(29) Latini, G.; Parrott, L. J.; Brovelli, S.; Frampton, M. J.; Anderson, H. L.; Cacialli, F. Cyclodextrin-threaded conjugated polyrotaxanes for organic electronics: The influence of the counter cations. *Adv. Funct. Mater.* **2008**, *18*, 2419–2427.

(30) Nyquist, R. M.; Ha, B. Y.; Liu, A. J. Counterion condensation in solutions of rigid polyelectrolytes. *Macromolecules* **1999**, *32*, 3481–3487.

(31) Antypov, D.; Holm, C. Osmotic coefficient calculations for dilute solutions of short stiff-chain polyelectrolytes. *Macromolecules* **2007**, *40*, 731–738.

(32) Blaul, J.; Wittemann, M.; Ballauff, M.; Rehahn, M. Osmotic coefficient of a synthetic rodlike polyelectrolyte in salt-free solution as a test of the Poisson-Boltzmann cell model. *J. Phys. Chem. B* **2000**, *104*, 7077–7081.

(33) Fuoss, R. M.; Katchalsky, A.; Lifson, S. The potential of an infinite rod-like molecule and the distribution of the counter ions. *Proc. Natl. Acad. Sci. U.S.A.* **1951**, *37*, 579–589.

(34) Alfrey, T.; Berg, P. W.; Morawetz, H. The counterions distribution in solutions of rod-shaped polyelectrolytes. *J. Polym. Sci.* **1951**, *7*, 543–547.

(35) Manning, G. S. Limiting laws and counterion condensation in polyelectrolyte solutions. 2. Self-diffusion of small ions. *J. Chem. Phys.* **1969**, *51*, 934–938.

(36) Oosawa, F. *Polyelectrolytes*; Marcel Dekker: New York, 1971.

(37) Ma, W. L.; Iyer, P. K.; Gong, X.; Liu, B.; Moses, D.; Bazan, G. C.; Heeger, A. J. Water/methanol-soluble conjugated copolymer as an electron-transport layer in polymer light-emitting diodes. *Adv. Mater.* **2005**, *17*, 274–277.

(38) Leaist, D. G.; Hao, L. Simultaneous measurement of mutual diffusion and intradiffusion by Taylor dispersion. *J. Phys. Chem. B* **1994**, *98*, 4702–4706.

(39) Moulins, J. R.; MacNeil, J. A.; Leaist, D. G. Thermodynamic Stability and the Origins of Incongruent and Strongly Coupled Diffusion in Solutions of Micelles, Solubilizates, and Microemulsions. *J. Chem. Eng. Data* **2009**, *54* (9), 2371–2380.

(40) Price, W. E. Theory of the Taylor dispersion technique for 3-component-system diffusion measurements. *J. Chem. Soc., Faraday Trans. I* **1988**, *84*, 2431–2439.

(41) Kelly, B.; Leaist, D. G. Using Taylor dispersion profiles to characterize polymer molecular weight distributions. *Phys. Chem. Chem. Phys.* **2004**, *6*, 5523–5530.

(42) Soderman, O.; Stilbs, P. NMR-Studies of complex surfactant systems. *Prog. Nucl. Magn. Reson. Spectrosc.* **1994**, *26*, 445–482.

(43) Mallavia, R.; Montilla, F.; Pastor, I.; Velasquez, P.; Arredondo, B.; Alvarez, A. L.; Mateo, C. R. Characterization and side chain manipulation in violet-blue poly-[(9,9-dialkylfluoren-2,7-diyl)-alt-co-(benzen-1,4-diyl)] backbones. *Macromolecules* **2005**, *38*, 3185–3192.

(44) Mallavia, R.; Martinez-Perez, D.; Chmelka, B. F.; Bazan, G. C. Blue fluorescent films based on poly-2,7-fluorene-phenylene derivatives. *Bol. Soc. Esp. Ceram. Vidrio* **2004**, *43*, 327–330.

(45) Chen, L. H.; McBranch, D.; Wang, R.; Whitten, D. Surfactant-induced modification of quenching of conjugated polymer fluorescence by electron acceptors: applications for chemical sensing. *Chem. Phys. Lett.* **2000**, *330*, 27–33.

(46) Molina, R. Ph. D. Thesis, Miguel Hernandez University Elche, Alicante, Spain, 2007.

(47) Barthel, J.; Gores, H. J.; Lohr, C. M.; Seidl, J. J. Taylor dispersion measurements at low electrolyte concentrations 0.1. Tetraalkylammonium perchlorate aqueous solutions. *J. Solution Chem.* **1996**, *25*, 921–935.

(48) Callendar, R.; Leaist, D. G. Diffusion coefficients for binary, ternary, and polydisperse solutions from peak-width analysis of taylor dispersion profiles. *J. Solution Chem.* **2006**, *35*, 353–379.

(49) Ribeiro, A. C. F.; Leaist, D. G.; Esteso, M. A.; Lobo, V. M. M.; Valente, A. J. M.; Santos, C.; Cabral, A.; Veiga, F. J. B. Binary mutual diffusion coefficients of aqueous solutions of beta-cyclodextrin at temperatures from 298.15 to 312.15 K. *J. Chem. Eng. Data* **2006**, *51*, 1368–1371.

(50) Deng, Z.; Leaist, D. G. Ternary mutual diffusion-coefficients of KCl-$LaCl_3$-water mixtures from Taylor dispersion profiles. *J. Solution Chem.* **1992**, *21*, 15–22.

(51) Packer, K. J.; Tomlinson, D. J. Nuclear spin relaxation and self-diffusion in binary system, dimethylsulfoxide (DMSO) + water. *Trans. Faraday Soc.* **1971**, *67*, 1302–1314.

(52) MacEwan, K.; Leaist, D. G. Incongruent diffusion (negative main mutual diffusion coefficient) for a ternary mixed surfactant system. *J. Phys. Chem. B* **2002**, *106*, 10296–10300.

(53) Hakansson, B.; Nyden, M.; Soderman, O. The influence of polymer molecular-weight distributions on pulsed field gradient nuclear magnetic resonance self-diffusion experiments. *Colloid Polym. Sci.* **2000**, *278*, 399–405.

(54) Chen, A.; Wu, D. H.; Johnson, C. S. Determination of molecular-weight distributions for polymers by diffusion-ordered NMR. *J. Am. Chem. Soc.* **1995**, *117*, 7965–7970.

(55) Nilsson, M.; Soderman, O.; Johansson, I. The effect of polymers on the phase behavior of balanced microemulsions: diblock-copolymer and comb-polymers. *Colloid Polym. Sci.* **2006**, *284*, 1229–1241.

(56) Sedlak, M.; Amis, E. J. Dynamics of moderately concentrated salt-free polyelectrolyte solutions - molecular-weight dependence. *J. Chem. Phys.* **1992**, *96*, 817–825.

(57) Zhao, T.; Beckham, H. W.; Ricks, H. L.; Bunz, U. H. F. Self-diffusion of poly(p-phenyleneethynylene)s in dilute solution determined by pulsed-field-gradient NMR. *Polymer* **2005**, *46*, 4839–4844.

(58) Knaapila, M.; Winokur, M. J. Structure and morphology of polyfluorenes in solutions and the solid state. *Adv. Polym. Sci.* **2008**, *212*, 227–272.

(59) Somma, E.; Loppinet, B.; Chi, C.; Fytas, G.; Wegner, G. Static and dynamic solution properties of monodisperse oligofluorenes. *Phys. Chem. Chem. Phys.* **2006**, *8*, 2773–2778.

(60) Riseman, J.; Kirkwood, J. G. The intrinsic viscosity, translational and rotatory diffusion constants of rod-like macromolecules in solution. *J. Chem. Phys.* **1950**, *18*, 512–516.

(61) LeBel, R. G.; Goring, D. A. I. Density, Viscosity, Refractive Index, and Hygroscopicity of Mixtures of Water and Dimethyl Sulfoxide. *J. Chem. Eng. Data* **1962**, *7*, 100–101.

(62) Gaylord, B. S.; Heeger, A. J.; Bazan, G. C. DNA hybridization detection with water-soluble conjugated polymers and chromophore-labeled single-stranded DNA. *J. Am. Chem. Soc.* **2003**, *125*, 896–900.

(63) Evans, D. F.; Wennerstrom, H. *The colloidal domain: where physics, chemistry, biology and technology meet*; Wiley-VCH: New York, 1999.

(64) Katchalsky, A. Polyelectrolytes. *Pure Appl. Chem.* **1971**, *26*, 327–373.

(65) Bordi, F.; Cametti, C.; Tan, J. S.; Boris, D. C.; Krause, W. E.; Plucktaveesak, N.; Colby, R. H. Determination of polyelectrolyte charge and interaction with water using dielectric spectroscopy. *Macromolecules* **2002**, *35*, 7031–7038.

(66) Nandi, P.; Das, B. Effects of concentration, relative permittivity, and temperature on the solution behavior of sodium carboxymethylcellulose as probed by electrical conductivity. *J. Phys. Chem. B* **2005**, *109*, 3238–3242.

(67) Rice, S. A. *Polyelectrolyte Solutions: A Theoretical Introduction*; Academic Press: New York, 1961; pp 83−89.

(68) Wagberg, T.; Liu, B.; Oradd, G.; Eliasson, B.; Edman, L. Cationic polyfluorene: conformation and aggregation in a “good” solvent. *Eur. Polym. J.* **2009**, *45*, 3230–3235.

Received for review October 23, 2009. Accepted January 4, 2010. MEC and FEDER are thanked for financial support through the project MAT2004-03827, MAT-2005-1004, MAT2008-06079/MAT, and POCI/FCT/FEDER through the project POCI/QUI/58291/2004. M.J.T. thanks Burgos University for financial support of a short stay in Coimbra University. C.I.A.V.S. is grateful for a Ph.D. Grant SFRH/BD/45669/2008 from Fundação para a Ciência e Tecnologia. H.D.B. thanks the FCT for a Sabbatical Leave Grant (SFRH/BSAB/886/2009), the Center for Photochemical Sciences at Bowling Green State University, and the Physics Department at Durham University for their hospitality.

JE900875W